Final Draft
of the original manuscript:

Ceylan Tuncaboylu, D.; Wischke, C.; Stoermann, F.; Lendlein, A.:
Microgels from microfluidic templating and photoinduced crosslinking of cinnamylidene acetic acid modified precursors
In: Reactive and Functional Polymers (2016) Elsevier

DOI: 10.1016/j.reactfunctpolym.2016.12.015

Microgels from microfluidic templating and photoinduced crosslinking of cinnamylidene acetic acid modified precursors

D. Ceylan Tuncaboylu[a,b,†], C. Wischke[a,†], F. Störmann[a], A. Lendlein[a]

[a] Institute of Biomaterial Science and Berlin-Brandenburg Centre for Regenerative Therapies, Helmholtz-Zentrum Geesthacht, Germany.

[b] Present address: Bezmialem Vakif University, Faculty of Pharmacy, 34-093 Istanbul, Turkey.

† Authors contributed equally.

Corresponding Author: A. Lendlein, Institute of Biomaterial Science, Helmholtz-Zentrum Geesthacht, Kantstr. 55, 14513 Teltow, Germany; Email: andreas.lendlein@hzg.de; Tel.: +49 (0)3328 352-450; Fax: -452.

Abstract

So far, a number of approaches to synthesize microgel networks have been followed, while only in few cases a detailed control of the network architecture has been possible. Here, the photoinduced [2 + 2] cycloaddition reaction of cinnamylidene acetic acid (CAA) moieties coupled to four-arm star shaped oligo(ethylene glycol) (OEG) precursors was explored for the creation of microgels with defined polymer network structures. Based on a rational solvent selection and precursor dispersion in glass-capillary microfluidics, microgels could be successfully prepared by the proposed synthesis approach. Model reactions confirmed a quantitative network formation. Therefore, compared to common radical polymerization for microgel crosslinking, CAA-dimerization may be an alternative approach particularly when well defined network structures are desired.

Keywords

Microgel, Cinnamylidene acetic acid, Photocrosslinking, Microfluidic

1 Introduction

Microgels are discrete sub-micrometer or micrometer-sized particles swollen in a suitable solvent, typically water, where the integrity of particles is preserved by an intraparticulate polymer network structure. The capacity of microgels to incorporate bioactive molecules or, when integrating stimuli-sensitive polymer segments, to switch their volume in response to suitable triggers has led to various concepts for drug delivery e.g. for peroral, parenteral or dermal application [1, 2]. The type and distribution of functional moieties in microgels can be of relevance for drug loading by electrostatic and hydrophobic interactions [3]. Beyond that, free reactive groups can enable further steps such as interparticulate crosslinks reported by disulfide exchange or by acrylate chemistry [4-6]. Considering these perspectives that arise from a control of functional moieties incorporated in microgels, defined crosslinking approaches are needed to build the polymer network structure.

So far, a number of approaches to synthesize microgel networks have been followed, including mixtures of comonomers and crosslinkers, oligomers functionalized with reactive moieties, or telechels enabling specific coupling reactions. Those approaches may lead to different levels of control over network structures.

Mixtures of (co)monomers with crosslinkers bearing at least two functional groups can be polymerized radically in an aqueous phase using acrylate or methacrylate chemistry, eventually leading to precipitation of typically submicron particles [7-10]. Irrespective whether this reaction is performed in a large volume of aqueous phase above the lower critical solution temperature as a soap-free emulsion polymerization or with addition of surfactants, or whether the polymerization is conducted in microdroplets templated e.g. by microfluidics, the chain segment length between netpoints and the netpoint functionality may only be statistically controlled by the (co)monomer-crosslinker ratio. Furthermore, different reactivities of (co)monomers and crosslinkers have been reported to cause inhomogeneities of microgels obtained by this strategy [7,11].

Oligomers or polymers functionalized with several lateral reactive moieties can be crosslinked in emulsion droplets, e.g. gelatin bearing methacrylate groups by photoinduced radical polymerization [12]. Again, the position of reactive moieties along the precursor chain and/or the number of chain segments connected per netpoint will follow a statistical distribution with limited possibility for control. Various biopolymer-based microgels, which form covalent networks with highly reactive crosslinkers like epichlorohydrin or physical networks e.g. upon interaction with ions or other charged components, may also fall into this category [13-15].

Microgels from oligomeric precursors of defined molecular weight and reactive endgroups for a specific coupling reaction have been reported recently. Some of these systems were based on a Michael addition of thiols to acrylates or on host-guest interaction or complexation e.g. of iron (II) ions by bipyridine moieties [16-18]. Such approaches may be best suited to obtain microgels with defined architectures. However, since cysteine in a cargo (e.g. protein encapsulation) may interfere with thiol-Michael addition and the supramolecular microgels may disintegrate upon dilution/ion extraction, alternative approaches in this category are of high interest.

This study should illustrate the principal suitability of building microgels with defined network structure using cinnamylidene acetic acid (CAA) moieties for specific coupling reactions. CAA was selected based on its capacity to undergo photoinduced [2 + 2] cycloaddition reaction [19, 20]. A two-phase droplet-based microfluidic dispersion technique [21], even if possibly not scalable to industrial applications without additional measures of parallelization or increase of the per-channel productivity [22,23,24], has been selected to obtain microgels with narrow size distributions. Furthermore, the reaction kinetics and conversion of CAA into dimers should be analyzed in model reactions to evaluate successful network formation.

2 Experimental

2.1 Materials

The materials were purchased as follows: four-arm oligo (ethylene glycol) (OEG, 5 kDa; PEGWorks, Winston-Salem, USA), cinnamylidene acetic acid (CAA; Alfa Caesar, Karlsruhe, Germany), oxalyl chloride (Acro Organics, Geel, Belgium), triethylamine (Carl Roth, Karlsruhe, Germany), tetrahydrofurane (Sigma Aldrich, Taufkirchen, Germany), *n*-Heptane (Merck, Darmstadt, Germany), D-α-Tocopheryl polyethylene glycol 1000 succinate (TPGS; Sigma, BioXtra), PVA (Mowiol® 4-88; 88% hydrolyzed, M_w = 12.6 kDa, polydispersity PD = 2.5), toluene (Sigma Aldrich, ACS Reagent, ≥99.5%), cyclohexane (for HPLC, ≥99.9%), *n*-butanol, chloroform, ethyl acetate (Merck, ACS Reagent).

2.2 Synthesis and characterization of PEG-CAA precursor

Four-arm star-shape OEG with hydroxyl endgroups (5 kDa; PEGWorks, Winston-Salem, USA) was molten in a dry flask in argon atmosphere at 65 °C. Cinnamylidene acetyl chloride, as synthesized by reaction of CAA and oxalyl chloride as reported before [20], and triethylamine were added at a 2.5 fold molar access compared to OEG endgroups and the reaction mixture was stirred in the dark for 3 d at 65 °C under argon atmosphere. The product was dissolved in dry tetrahydrofurane and, after filtration, precipitated into cold *n*-heptane. This process was repeated three times and then the OEG-CAA was dried in vacuum at room temperature.

Fourier-transform infrared spectroscopy (FTIR) spectra were recorded by a Nicolet 6700 spectrometer (Thermo Scientific, Waltham, USA) in attenuated total reflection (ATR) mode. The sample measurement was performed with 50 scans and a resolution of 4 cm^{-1} (Suppl. Fig. 1).

^{1}H-NMR spectroscopy in $CDCl_3$ (500 MHz Avance spectrometer, Bruker, Rheinstetten, Germany) was applied to confirm the CAA functionalization. The degree of OEG-CAA functionalization was calculated to be 0.87 based on the ratio between the signals corresponding to CAA (δ = 6.03; 6.8-7.1; 7.29-7.67 ppm) and the pentaerythritol core of OEG (δ = 3.41 ppm) (Suppl. Fig. 2).

2.3 Screening of OEG-CAA solubility and emulsification tests

Solubility tests of the OEG-CAA were conducted in test tubes using various solvents, where 10% (w/v) was the target concentration. In order to screen the capability for emulsification, 10% (w/v) solution of the precursor was dropped into a test tube containing either 5% (w/v) of aqueous PVA solution or 0.3% (w/v) of TPGS at a volume ratio of organic phase and continuous phase of 1:10 with subsequent vortexing (30 s). The emulsion was transferred into a 10 mL beaker, irradiated under magnetic steering for 30 min (Omnicure, 320-480 nm, 4 cm distance), and transferred into 75 mL water with overnight stirring for solvent evaporation. Droplet and particle appearance was examined microscopically.

The solubility parameters were calculated with the HSPiP software based on Yamamoto molecular breaking group contribution method.

2.4 Design and operation of glass capillary microfluidic devices for droplet templating

Microfluidic devices of flow-focusing geometry were assembled with epoxy glue on a glass slide using two types of borosilicate glass capillaries (Hilgenberg, Malsfeld, Germany): outer capillaries of square shape (outside dimension 1.35 mm, inside 1.1 mm) and inner capillaries of circular cross section (outer diameter 1.0 mm, inner diameter 0.58 mm). The inner capillaries were tapered by a micropipette puller (P-1000, Sutter Instruments) to orifice sizes of ~200 μm. The devices were operated in dripping conditions by feeding 10% (w/v) OEG-CAA solution in $CHCl_3$ as o-phase to the inner capillary and 5% (w/v) PVA as w-phase to the outer capillary at different flow rates (Suppl. Fig. 3). Polyethylene tubing was used to connect the syringe pumps (AL 1010, WPI) and the device. Droplet formation was monitored by a digital high-speed microscope (VW 6000E with VH-Z100R lens and VW 100C camera, Keyence Deutschland GmbH, Neu-Isenburg, Germany).

2.5 Microgel crosslinking and imaging

Templated OEG-CAA droplets were collected either in a beaker with PVA solution or, preferentially, in a reaction chamber composed of a metallic frame with two quartz glass plates with a distance of 2 mm to avoid solvent evaporation (see Suppl. Fig. 4). Crosslinking of OEG-CAA to microgels was achieved by means of UV irradiation (OmniCure S2000), where the light guide was placed at 5 cm distance to illuminate the chamber (0.3 $W \cdot cm^{-2}$). An optical microscope (DMI6000B, Leica, Wetzlar, Germany) was used to image the collected droplets before and after crosslinking.

Freshly prepared particles were examined by environmental scanning electron microscopy (ESEM; FEI Quanta FEG 250 including EDX X-ray analysis). The images were obtained at 2 °C using a gaseous secondary electron detector with a changing pressure of the sample chamber and an accelerating voltage of 10 kV. A benchtop scanning electron microscope (SEM; Phenom G2 pro, Eindhoven, Netherlands) was also used for particle imaging. Prior to the SEM analysis, collected particles were dispersed on a silica wafer by a spin coater and then sputter-coated with 5 nm gold using Quorum Q 150 T ES (Gala Instruments).

2.6 Model reactions of OEG-CAA crosslinking

Model reactions were carried out in the rheometer (Physica MCR 301 Anton Paar, Germany), which is equipped with a 320-480 nm UV lamp (S2000, OmniCure, Mississauga, Canada). A plate-plate setup (diameter 25 mm; initial distance 500 μm) was used in oscillatory mode at 24 °C with a solvent trap to minimize the evaporation. A frequency of ω = 1 Hz and a deformation amplitude γ_0 = 0.01 were selected, which correspond to conditions where the oscillatory deformation was in the linear regime.

2.7 Precision of instrumental techniques and statistics

The precision of quantitative analysis by NMR is typically expected to be in the range of 3-5%. Syringe pumps have a dispersion accuracy of ± 1%. Particle sizes are stated as mean ± standard deviation from n > 100 particles as determined from light microscopy images.

3 Results and discussion

3.1 Crosslinking concept, solvent selection and microfluidic templating

In order to prepare microgels with defined network architectures, star-shaped telechels were employed in combination with CAA endgroups as they are known to undergo a [2 + 2] cycloaddition reaction under UV irradiation of λ > 254 nm [19]. Accordingly, as illustrated in Fig. 1, junction units are formed by CAA dimers, while the central carbon of the polymeric precursor acts as netpoint. Thus, upon complete crosslinking, network properties will be highly defined by the arm length of the telechels. According to the aim of this study to principally illustrate a successful microgel formation, a four-arm star shaped OEG precursor of 5 kDa was selected, functionalized with CAA (OEG-CAA, degree of functionalization 0.87) and employed in microgel synthesis.

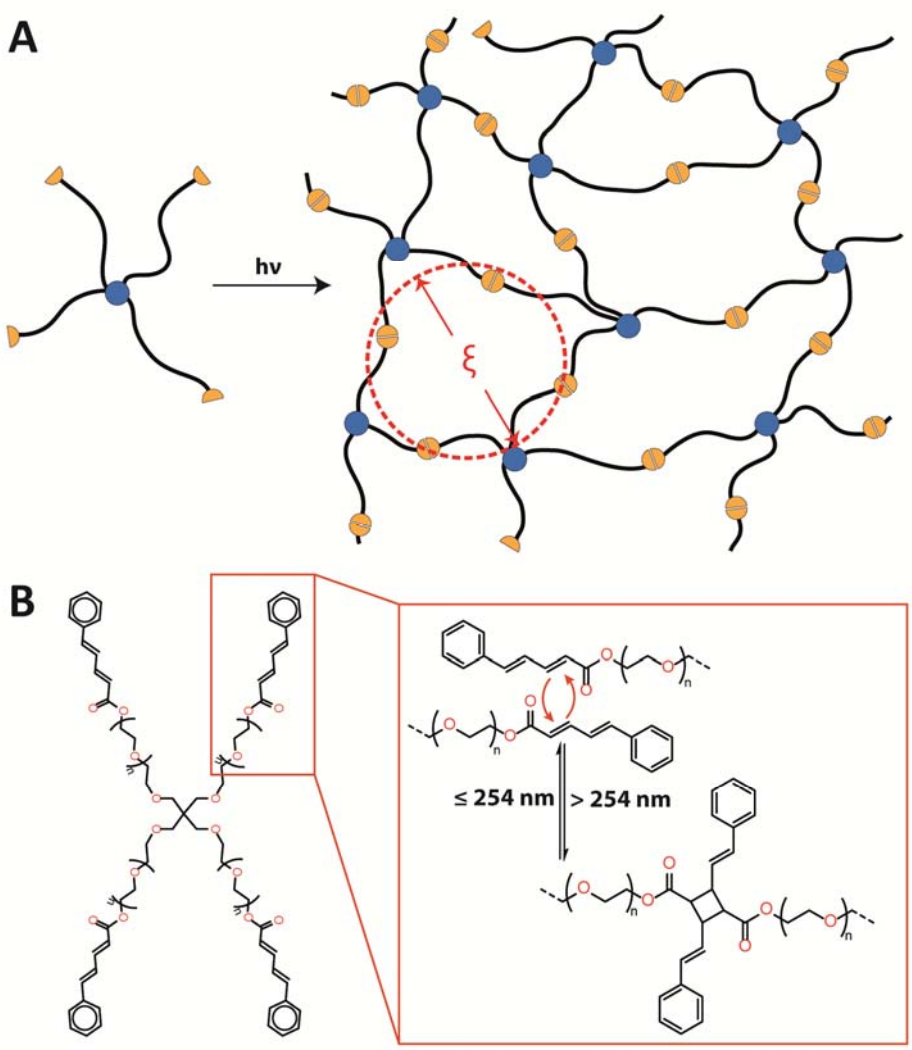

Fig. 1: Scheme of polymer network structure obtained upon precursor crosslinking (Note: For easier visibility, the scheme shows a simplified 2-dimensional plot. The four-arm precursors will acquire a 3-dimensional orientation and in contrast to ideal networks, experimental polymer networks may include e.g. dangling chains or chain entanglements.)

First, the telechel solution should be dispersed into droplets that then serve as microreactors for subsequent precursor crosslinking into individual microgel particles. For the disperse phase, a solvent had to be employed, which would provide (i) suitable solubility of OEG-CAA, (ii) immiscibility with the continuous phase to allow o/w (organic phase in water phase) emulsification, (iii) a low water uptake to prevent water influx into the precursor droplets that may affect polymer network synthesis and structure, and (iv) temporal stability of the o/w emulsion until the subsequent crosslinking process is completed. Table 1 summarizes the properties of solvents that were selected based on their decreasing water uptake as well as their Hansen solubility parameters comprising δ_d, δ_p, and δ_H, which correspond to energy from dispersion forces, dipolar interaction and hydrogen bonds, respectively. For Ethyl-

[1]OEG-CAA, corresponding to the structure of one OEG-CAA arm and roughly serving here to estimate the precursor molecules, δ_d = 16.5 $MPa^{1/2}$, δ_p = 4 $MPa^{1/2}$ and δ_H = 8 $MPa^{1/2}$ have been calculated. It was obvious that particularly those solvents with very low water uptake and low contribution of δ_p and δ_H were insufficient o-phase solvents, as can be seen both from distance R_a of solute (Ethyl-[1]OEG-CAA) and solvent in the Hansen space as well as the experimental dissolution data (Table 1). For OEG-CAA solutions in ethyl acetate, chloroform or toluene, the stability of o/w emulsions in an aqueous continuous phase was studied comparing different stabilizer types and concentrations (see Supporting Information, Table S1). Only in case of OEG-CAA in chloroform dispersed in aqueous polyvinyl alcohol (PVA) solution, a stable droplet formation was observed.

Table 1: Solvents evaluated for OEG-CAA dissolution based on limited water-miscibility, Hansen solubility parameters, and experimental polymer dissolution as well as emulsification tests.

Solvent of o-phase	o-phase Solubility (wt.%) [a]		Hansen solubility parameter [b]				OEG-CAA dissolution [c]	Stabile droplet/ particle formation[d]
	Solvent /Water	Water/ Solvent	δ_d ($MPa^{1/2}$)	δ_p ($MPa^{1/2}$)	δ_h ($MPa^{1/2}$)	R_a ($MPa^{1/2}$)		
Ethyl acetate	7.7	3.3	15.8	5.3	7.2	2.1	✓	×
Chloroform	0.82	0.072	17.8	3.1	5.7	3.6	✓	✓
Toluene	0.05	0.033	18.0	1.4	2.0	7.2	✓	×
Cyclohexane	0.01	0.0055	16.8	0	0.2	8.8	×	n.a.
n-Hexane	0.001	0.011	14.9	0	0	9.5	×	n.a.
n-Heptane	0.0003	0.010	15.3	0	0	9.3	×	n.a.

n.a. = not applicable.

[a] Data from [30].

[b] Hansen solubility parameter calculated by HSPiP software; linear Ethyl-[1]OEG-CAA ($\delta_{d,1}$ = 16.5 $MPa^{1/2}$, $\delta_{p,1}$ = 4 $MPa^{1/2}$, $\delta_{H,1}$ = 8 $MPa^{1/2}$) was used as mimic of star-shaped OEG-CAA; $(R_a)^2 = 4(\delta_{d,2} - \delta_{d,1})^2 + (\delta_{p,2} - \delta_{p,1})^2 + (\delta_{h,2} - \delta_{h,1})^2$ describing distance R_a of solute and solvent in the Hansen space.

[c] Precursors were considered as soluble when 10% (w/v) of OEG-CAA could be dissolved in the respective solvent at room temperature.

[d] Emulsification with 10% (w/v) OEG-CAA in given solvent; continuous phase 5% (w/v) PVA; for details see Suppl. Table 1.

In order to prepare defined sizes of pre-microgel templates, a microfluidic dispersion technique was applied. The microfluidic device was constructed from glass capillaries and operated in the flow-focusing mode using syringe pumps to provide the two phases [21]. The o/w emulsification of OEG-CAA/chloroform phase in the continuous PVA/water phase, as previously seen in batch emulsification, could also be reproduced

in the continuous microfluidic process. When the flow rates of the continuous phase Q_w where increased while keeping the o-phase flow rates Q_o constant, the droplet size could be systematically varied, e.g. ~130 µm at a Q_o/Q_w = 0.14 (Fig. 2). This can be assigned to the increasing shear at the orifice and the tapering of the jet of the precursor solution. It should be noted that microscopic analysis of droplet size indicated a very narrow size distribution with some variation probably arising from pulsate flow typically associated with syringe pumps [25].

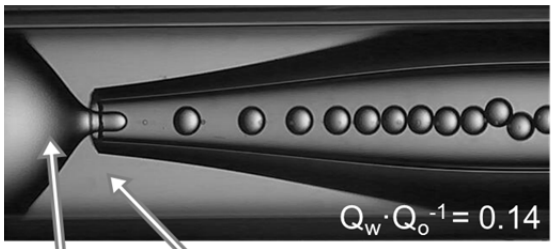

Q_w w-phase [µl·min^{-1}]	Q_o o-phase [µl·min^{-1}]	$Q_w \cdot Q_o^{-1}$	Droplet size [µm]
19	140	0.14	135 ± 5
19	190	0.10	110 ± 5
19	280	0.07	75 ± 5

Fig. 2: Effect of flow rates on the droplet size of o/w emulsions from microfluidic droplet templating (further images in Suppl. Information). Experiments were conducted with a glass capillary device with 210 µm orifice operated in flow focusing mode, using 10% (w/v) OEG-CAA in chloroform as o-phase and 5% (w/v) PVA as continuous w-phase.

3.2 Microgel synthesis by in-droplet crosslinking

While appropriate condition to template droplets (e.g. ~ 130 µm) in the microfluidic channel have been identified as described above, the droplets now had to be subjected to gelation by CAA crosslinking. It should be noted that attempts of an integrated process with in-channel crosslinking were not successful with the available equipment because only a limited UV exposure time could be realized even in long channels with meander-shaped structure. Accordingly, a batch process should be applied, where droplets were collected in a cell composed of a metal frame and two quartz glass plates with a distance of 2 mm (see Suppl. Fig. 4) and irradiated in this closed system. When applying an Excimer lamp as intense UV source characterized by roughly monochromatic light (here 308 nm, 0.08 W·cm^{-2}), which is within the range of light reported before (300-400 nm [19]), no crosslinking was observed even when changing to model reactions with films and irradiation times up to 30 min. This

suggests that the nearly monochromatic light source of 308 nm may not be sufficient to induce CAA [2 + 2] cycloaddition in this system. Accordingly, a UV lamp with a broader emission range (320-480 nm, 0.3 $W \cdot cm^{-2}$) was applied.

Fig. 3 summarizes the droplet morphology at different stages of the successful microgel synthesis. The templated droplets where of homogenous structure and had sizes of 107 ± 8 µm (Fig. 3A-B). Importantly, after crosslinking and exchange of the solvent by $CHCl_3$ extraction/evaporation, the integrity of microgels in water confirmed successful crosslinking (Fig. 3C). The water-swollen microgels had sizes of 120 ± 17 µm, not considering the few very small particles visible in Fig. 3C, which may be satellite particles from microfluidic dispersion or droplet splitting by turbulences at the inlet of the quartz glass reactor. The size distribution of crosslinked microgels in water was slightly larger compared to pre-gel droplets (Fig. 3B,C), which may be due to different UV light intensities and crosslinking in different positions of the quartz glass reactor. In contrast to the templated OEG-CAA solution droplets, whose size (107 ± 8 µm) was defined by the microfluidic process, the microgel size of 120 ± 17 µm can be considered as an equilibrium swollen state of the microgel network in water. In the dried state, the particles were substantially smaller as seen in additional SEM analysis (Fig. 3 D-E).

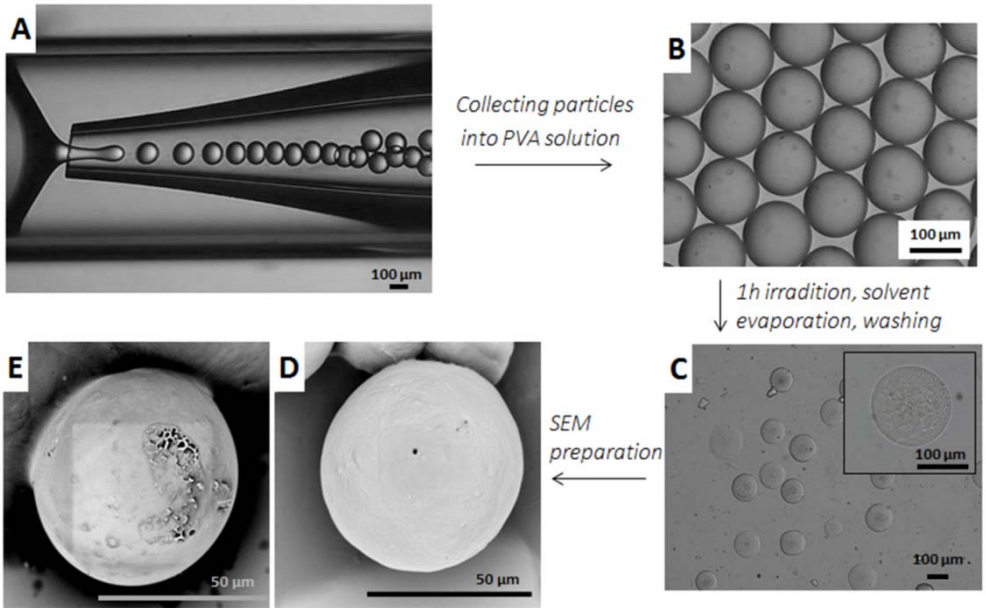

Fig. 3: Particle collection and crosslinking in a quartz glass cell. (A) Templating of homogeneously sized droplets. (B) Droplets collected from microfluidic device. (C) Water-swollen microgels after crosslinking in the quartz glass cell, overnight steering in beaker for $CHCl_3$ removal, and washing steps. (D, E) Particle images obtained by SEM (dry state). Preparation conditions were: o-phase 10% w/v OEG-CAA in $CHCl_3$, w-phase 5% w/v PVA in water, orifice size 200 µm, flow rates $Q_o/Q_w = 0.14$; $Q_o = 35$ µl/min; 1 h irradiation (320-480 nm) for crosslinking.

Light microscopy suggested some internal structuring of the microgels, which might be cavities formed by water influx during the crosslinking process (compare Table 1, water solubility in $CHCl_3$). SEM images indicated that the microgels had an apparently closed surface structure, but might be macroporous in their core (Fig. 3D-E). Since macroporous, covalently crosslinked gels with structured pores have before been shown to very well recover from mechanical deformation, this might be an advantageous and possibly application relevant feature [26, 27].

The capacity of these microgels to swell in both organic solvents and aqueous media is an interesting feature. In order to further characterize the microgels, an in situ dehydration/hydration study was performed by ESEM. When the relative humidity of the gaseous environment was decreased e.g. from 100% to 91.6%, the diameter of a microgel particle decreased from 122 µm to an equilibrated size of 111 µm within < 5 min (25% volume loss). This instantaneous particle shrinkage (as well as swelling upon increasing humidity) suggests rapid hydration/dehydration kinetics.

In order to further evaluate the formation of a defined network structure during the crosslinking reaction, rheological examination of thin films as model matrices was conducted. Specifically, by using the same UV source coupled into the rheometer, the crosslinking kinetics could be additionally monitored. Since covalent crosslinking is associated with conversion from a predominantly viscous to a viscoelastic material, the time of gelation can be assigned to the condition when the storage modulus G' exceeds the loss modulus G'' (crossover point). This condition has been reached when irradiating the OEG-CAA solution for 15 min (Fig. 4A). The visual examination of isolated films confirmed successful gelation. However, it should be noted that the crossover point does not reflect the state of a fully crosslinked material. Further irradiation illustrated that G'' adapted a plateau after ~30 min and G' reached a similar state afterwards. Considering the here applied principle of network formation as described above and highlighted in Fig. 1, a quantitative conversion of the four endgroups of each precursor molecule would lead to a situation where the concentration of netpoints equals the concentration of telechels employed in a given volume (neglecting possible additional netpoints from physical entanglements). Based on the correlation of mechanical properties and network architecture for ideal polymer networks, the average mesh size ξ and netpoint density ν_c can be calculated according to Eqs. 1-2 [28,29].

$$\nu_c = \frac{G'}{R \cdot T} \qquad (1)$$

$$\xi = \left(\frac{G' \cdot N_A}{R \cdot T}\right)^{-1/3} \qquad (2),$$

where R is the universal gas constant, T is the absolute temperature, and N_A is the Avogadro constant.

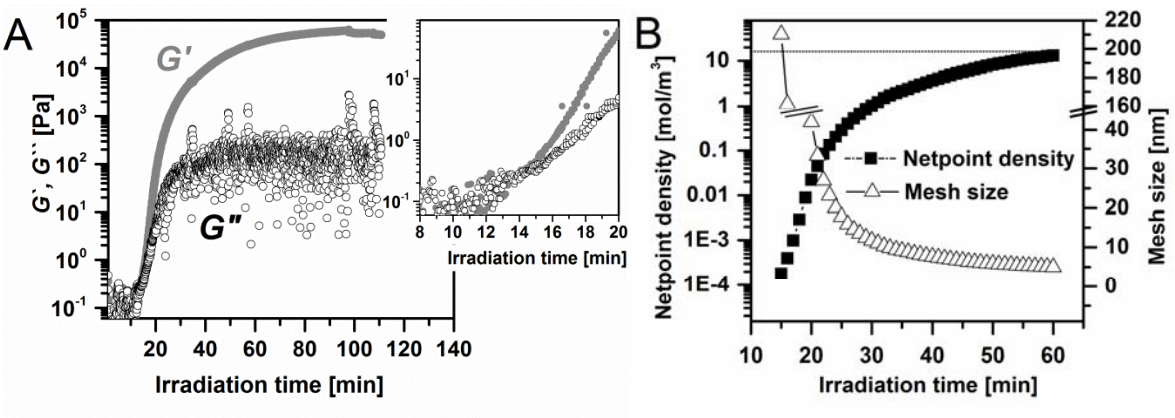

Fig. 4: Model reaction studying gel formation by rheology as a function of irradiation time. (A) Elastic modulus G' (●) and viscous modulus G'' (○) during the crosslinking of 10% (w/v) OEG-CAA in $CHCl_3$. Insert shows crossover point. ω = 1 Hz, γ = 0.01. (B) Analysis of kinetic changes of netpoint density (■) and mesh size (△) with irradiation time as calculated from rheological data. The dashed line corresponds to the theoretical netpoint density for the ideal case of 100% conversion with telechels showing a d_f of 100% (here: d_f 87%). The irradiation was conducted at 320-480 nm.

It could be shown that mesh sizes substantially decrease from > 200 nm at 15 min to ~5 nm after 60 min (Fig. 4B). Simultaneously, the netpoint density increased gradually from 0.0002 to 13.2 mol·m^{-3}, which is very close to the theoretical maximum value for an ideal case scenario with 100% conversion (~16.3 mol·m^{-3}) as calculated from the precursor concentration employed in the reaction. A quantitative conversion has also been reported in the literature [19]. Small discrepancies may be assigned to the precision of the method, the slightly reduced degree of OEG functionalization with CAA endgroups (d_f 87%) or possible side reactions that may have consumed some of the CAA moieties (e.g. photolysis of $CHCl_3$ to highly reactive species).

Overall, the presented data from various characterization techniques strongly support that microgels with well-defined network architectures can be obtained by using CAA dimerization as a novel synthesis approach for microgels. The microgels appeared stable during handling, exchange of swelling agent from chloroform (during synthesis) to water and ESEM experiments with reversible shrinkage and expansion without alteration of outer particle appearance.

4 Conclusions

Microgels with defined polymer network architecture were successfully prepared in this study, synthesized from telechelic precursors by a [2 + 2] cycloaddition reaction. This specific coupling reaction, so far not considered for microgels, can be assumed to provide nearly ideal networks based on the determined netpoint density. Therefore, compared to common radical polymerization for microgel crosslinking, CAA-dimerization may be an alternative approach and a platform for various future studies, particularly when well defined network structures are desired.

Acknowledgements

The authors acknowledge Daniela Radzik for precursor synthesis and Prof. Dr. Steven Abbott for calculating the Hansen solubility parameters. The Helmholtz Association within programme-oriented funding, the Federal Ministry of Education and Research, Germany, within the Framework Programme Health Research (grant No. 1315848A and No. 13GW0098), and the German Research Council through the Collaborative Research Center 1112, subproject A03, are acknowledged for partial funding.

Appendix A. Supplementary data

Supplementary Information is provided showing in Suppl. Fig. 1-4 the FTIR spectrum and ^{1}H-NMR spectrum of OEG-CAA, the images of microfluidic dispersion at different flow conditions, and the experimental setup for photocrosslinking the microgels. In Suppl. Table 1, the screening of o/w emulsion stability is summarized.

References

[1] H. Bysell, R. Mansson, P. Hansson, M. Malmsten, Adv Drug Deliver Rev, 63 (2011) 1172-1185.
[2] V.C. Lopez, J. Hadgraft, M.J. Snowden, Int. J. Pharm., 292 (2005) 137-147.
[3] T. Hoare, R. Pelton, Langmuir, 24 (2008) 1005-1012.
[4] J.C. Gaulding, M.H. Smith, J.S. Hyatt, A. Fernandez-Nieves, L.A. Lyon, Macromolecules, 45 (2012) 39-45.
[5] A.H. Milani, A.J. Freemont, J.A. Hoyland, D.J. Adlam, B.R. Saunders, Biomacromolecules, 13 (2012) 2793-2801.
[6] T. Lane, J.L. Holloway, A.H. Milani, J.M. Saunders, A.J. Freemont, B.R. Saunders, Soft Matter, 9 (2013) 7934-7941.
[7] X. Wu, R.H. Pelton, A.E. Hamielec, D.R. Woods, W. McPhee, Colloid Polym. Sci., 272 (1994) 467-477.

[8] D. Sivakumaran, D. Maitland, T. Oszustowicz, T. Hoare, J Colloid Interf Sci, 392 (2013) 422-430.
[9] S. Aerry, A. De, A. Kumar, A. Saxena, D.K. Majumdar, S. Mozumdar, J. Biomed. Mater. Res. A, 101 (2013) 2015-2026.
[10] F. Schneider, A. Balaceanu, A. Feoktystov, V. Pipich, Y.D. Wu, J. Allgaier, W. Pyckhout-Hintzen, A. Pich, G.J. Schneider, Langmuir, 30 (2014) 15317-15326.
[11] T. Still, K. Chen, A.M. Alsayed, K.B. Aptowicz, A.G. Yodh, J Colloid Interf Sci, 405 (2013) 96-102.
[12] C.E.Y. Cha, J. Oh, K. Kim, Y.L. Qiu, M. Joh, S.R. Shin, X. Wang, G. Camci-Unal, K.T. Wan, R.L. Liao, A. Khademhosseini, Biomacromolecules, 15 (2014) 283-290.
[13] W.F. Zhao, R.W.N. Nugroho, K. Odelius, U. Edlund, C.S. Zhao, A.C. Albertsson, Acs Appl Mater Inter, 7 (2015) 4202-4215.
[14] Y.D. Hu, G. Azadi, A.M. Ardekani, Carbohyd Polym, 120 (2015) 38-45.
[15] Y. Huang, Y. Lapitsky, Langmuir, 27 (2011) 10392-10399.
[16] H.J. Zhang, Y. Xin, Q. Yan, L.L. Zhou, L. Peng, J.Y. Yuan, Macromol Rapid Comm, 33 (2012) 1952-1957.
[17] T. Rossow, S. Bayer, R. Albrecht, C.C. Tzschucke, S. Seiffert, Macromol Rapid Comm, 34 (2013) 1401-1407.
[18] Y.Z. Yin, S.F. Jiao, R.R. Zhang, X.X. Hu, Z.F. Shi, Z.Q. Huang, Soft Matter, 11 (2015) 5301-5312.
[19] F.M. Andreopoulos, C.R. Deible, M.T. Stauffer, S.G. Weber, W.R. Wagner, E.J. Beckman, A.J. Russell, J. Am. Chem. Soc., 118 (1996) 6235-6240.
[20] C. Melchert, N. Yongvongsoontorn, M. Behl, A. Lendlein, J Appl Biomater Func, 10 (2012) 185-190.
[21] R.K. Shah, H.C. Shum, A.C. Rowat, D. Lee, J.J. Agresti, A.S. Utada, L.Y. Chu, J.W. Kim, A. Fernandez-Nieves, C.J. Martinez, D.A. Weitz, Mater. Today, 11 (2008) 18-27.
[22] T. Nisisako, T. Ando, T. Hatsuzawa, Lab Chip, 12 (2012) 3426-3435.
[23] W. Li, E.W.K. Young, M. Seo, Z. Nie, P. Garstecki, C.A. Simmons, E. Kumacheva, Soft Matter, 4 (2008) 258-262.
[24] S. Seiffert, F. Friess, A. Lendlein, C. Wischke, J. Colloid Interface Sci., 452 (2015) 38-42.
[25] Z. Li, S.Y. Mak, A. Sauret, H.C. Shum, Lab Chip, 14 (2014) 744-749.
[26] S.A. Bencherif, R.W. Sands, D. Bhatta, P. Arany, C.S. Verbeke, D.A. Edwards, D.J. Mooney, P Natl Acad Sci USA, 109 (2012) 19590-19595.
[27] A.T. Neffe, B.F. Pierce, G. Tronci, N. Ma, E. Pittermann, T. Gebauer, O. Frank, M. Schossig, X. Xu, B.M. Willie, M. Forner, A. Ellinghaus, J. Lienau, G.N. Duda, A. Lendlein, Adv. Mater., 27 (2015) 1738-1744.
[28] P.B. Welzel, S. Prokoph, A. Zieris, M. Grimmer, S. Zschoche, U. Freudenberg, C. Werner, Polymers-Basel, 3 (2011) 602-620.
[29] A. Hajighasem, K. Kabiri, J. Polym. Res., 20 (2013) 218.
[30] I.M. Smallwood, Handbook of Organic Solvent Properties, Arnold, London, Great Britain, 1996.